

In situ characterization of CD4⁺ T cell behavior in mucosal and systemic lymphoid tissues during the induction of oral priming and tolerance

Bernd H. Zinselmeyer,^{1,2} John Dempster,³ Alison M. Gurney,^{2,3} David Wokosin,² Mark Miller,⁴ Hsiang Ho,⁴ Owain R. Millington,¹ Karen M. Smith,¹ Catherine M. Rush,¹ Ian Parker,⁵ Michael Cahalan,⁴ James M. Brewer,¹ and Paul Garside¹

¹Division of Immunology, Infection, and Inflammation, University of Glasgow, Western Infirmary, Glasgow G11 6NT, Scotland, UK

²Centre for Biophotonics and ³Department of Physiology and Pharmacology, University of Strathclyde, Glasgow G4 0NR, Scotland, UK

⁴Department of Physiology and Biophysics and ⁵Department of Neurobiology and Behavior, University of California, Irvine, CA 92697

The behavior of antigen-specific CD4⁺ T lymphocytes during initial exposure to antigen probably influences their decision to become primed or tolerized, but this has not been examined directly in vivo. We have therefore tracked such cells in real time, in situ during the induction of oral priming versus oral tolerance. There were marked contrasts with respect to rate and type of movement and clustering between naive T cells and those exposed to antigen in immunogenic or tolerogenic forms. However, the major difference when comparing tolerized and primed T cells was that the latter formed larger and longer-lived clusters within mucosal and peripheral lymph nodes. This is the first comparison of the behavior of antigen-specific CD4⁺ T cells in situ in mucosal and systemic lymphoid tissues during the induction of priming versus tolerance in a physiologically relevant model in vivo.

CORRESPONDENCE

Paul Garside:
paul.garside@clinmed.gla.ac.uk
OR

Michael Cahalan:
mcahalan@uci.edu

Abbreviations used: CFSE, carboxyl fluorescein succinimidyl ester; CLN, cervical LN; CT, cholera toxin; MLN, mesenteric LN; PLN, peripheral LN; SMAC, supramolecular cluster; Tg, transgenic.

The basis of the dichotomy in immune responsiveness between tolerance and immunity remains elusive. Recent in vivo studies have shown that these two very different outcomes are both the result of initial activation and clonal expansion of antigen-specific T cells after cognate interaction between a naive T cell and an APC (1, 2). However, how the process diverges to produce the distinct immunological phenotypes of immunity versus tolerance remains unclear. Several in vitro, and more recently in vivo, studies have shown that initial contact between recirculating naive T cells and APCs occurs in a nonspecific manner via low-affinity interactions, which progress to a more stable “immunological synapse” or supramolecular cluster (SMAC) upon recognition of an appropriate peptide–MHC combination (3–5). It remains controversial whether productive activation of an antigen-specific T cell results from a single, long-lived encounter of this type or oc-

curs after frequent short-lived encounters (serial encounter model; references 3–6), and differences in the duration and/or frequency of interactions between APCs and T cells have also been proposed to underlie the outcome of priming versus tolerance (3). This suggestion was based on a number of elegant studies (using two-photon excitation microscopy; references 7–15), which have defined marked differences in behavior between naive and antigen-exposed T cells in real-time in situ (7–15). However, such analyses of CD4⁺ T cells during the induction of tolerance have not been undertaken and their behavior remains undefined. We have therefore characterized the behavior of antigen-specific CD4⁺ T cells in local and systemic lymphoid tissues in situ after feeding antigen in a physiologically relevant system of immunoregulation that we and others have previously shown to be a robust and reproducible model of peripheral priming and tolerance, which exposes marked effects on parameters ranging from proliferation and cytokine production in vitro to antibody

The online version of this article contains supplemental material.

production, delayed-type hypersensitivity responses, T cell migration, and help for B cells *in vivo* (2, 16–19).

RESULTS

As expected, two-photon excitation microscopy of mesenteric LNs (MLNs) draining the gastrointestinal tract and peripheral LNs (PLNs) after the induction of priming and tolerance (Fig. 1 a) demonstrated that carboxyl fluorescein succinimidyl ester (CFSE)-labeled, antigen-specific T cells could be detected in these lymphoid organs (Fig. 1). In general, their numbers appeared to increase upon exposure to antigen (Fig. 1, c, d, f, g, i, j, l, and m), consistent with observations by conventional immunohistochemistry (2). To directly compare T cell behavior in naive, primed, and tolerized animals, the volume and location of each cell was measured in 21 planes per three-dimensional stack of $222 \times 178\text{-}\mu\text{m}$ optical sections collected at $2.5\text{-}\mu\text{m}$ intervals be-

tween each plane progressing deeper into the LN from an initial depth of $\sim 100\text{ }\mu\text{m}$ below the surface. The time interval between each stack was 18 s.

In general, naive T cells (Fig. 1, b, e, h, and k) displayed an apparently wandering, random walk behavior (Videos 1, 4, 7, 10, available at <http://www.jem.org/cgi/content/full/jem.20050203/DC1>), consistent with previous papers (7–15). This was observed in the MLNs and cervical LNs (CLNs), the latter examined as a representative PLN, at both 8 and 20 h after animals were fed vehicle alone. Comparisons of local (MLNs) and PLNs were made throughout our studies as the effects of fed antigen upon systemic immune responses remain controversial and unclear.

Observation of the induction of CD4⁺ T cell priming

Induction of priming by oral administration of immunogenic antigen with cholera toxin (CT) adjuvant led to dramatic

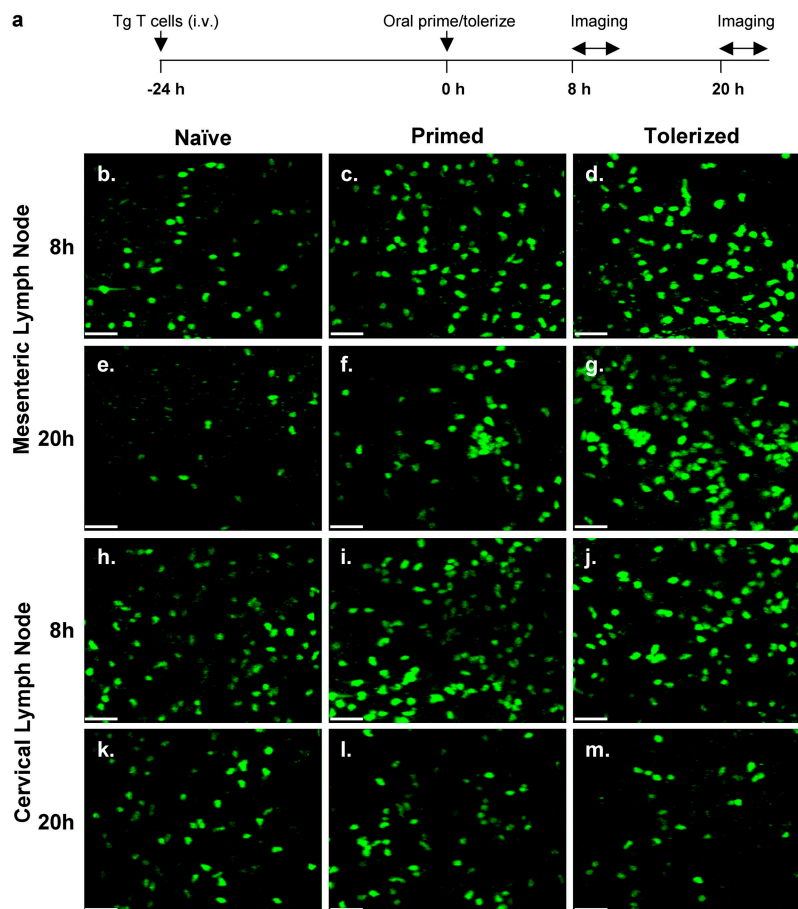


Figure 1. Observation of antigen-specific T cells in local and PLNs at various times during the induction of oral priming versus oral tolerance. BALB/c mice were adoptively transferred with CFSE-labeled, DO11.10 T cells and remained naive or were fed 100 mg OVA + 20 μg CT or 100 mg OVA (a). Mesenteric (b–g) and CLNs (h–n) were removed 8 h (b–d, h–j) and 20 h (e–g, k–n) after feeding PBS (b, e, h, and k), OVA + CT (c, f, i, and l) or OVA alone (d, g, j, and n) and imaged as described in Mate-

rials and methods. Images shown are z-projections of 21 sequential image stacks $2.5\text{ }\mu\text{m}$ apart and are representative of those seen in at least three fields of view in at least two to three animals per group. Movement of T cells is shown in Videos 1–12. Replicate experiments were performed at the University of Strathclyde and at the University of California, Irvine with similar findings; those from the latter are shown.

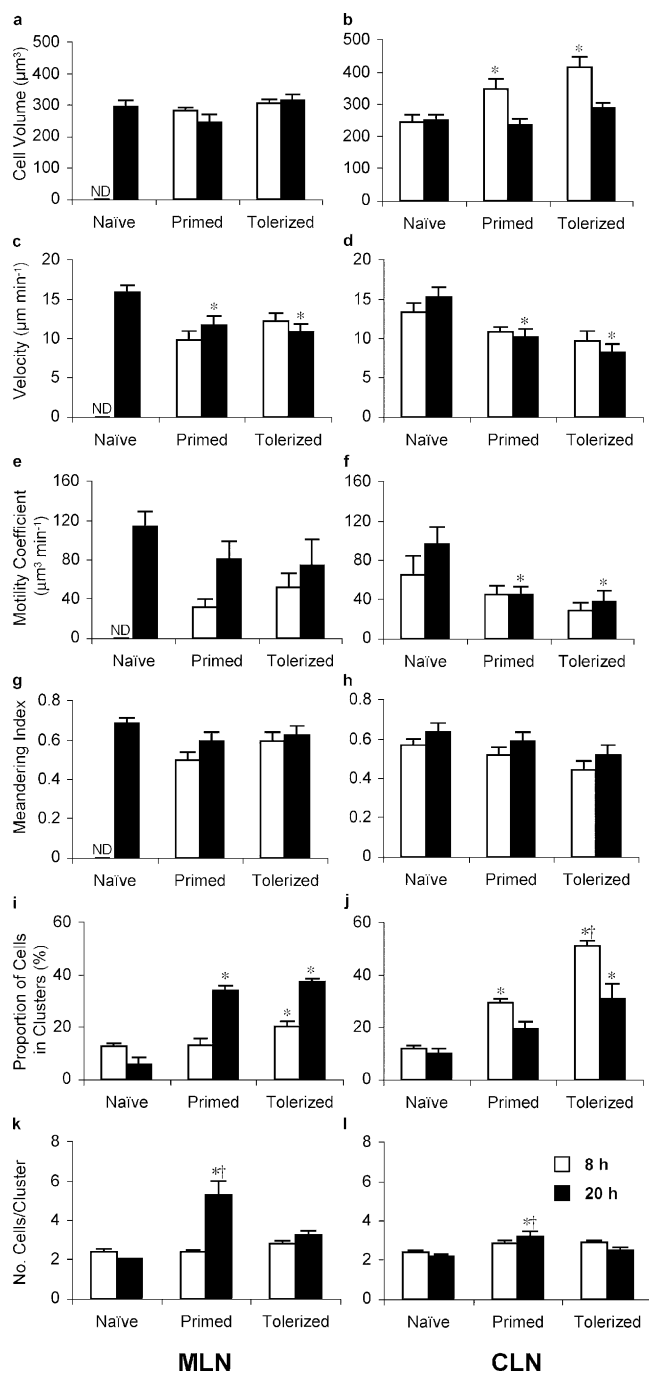


Figure 2. Analysis of the behavior of antigen-specific T cells in MLNs during the induction of oral priming and tolerance. As described in Fig. 1, BALB/c mice were adoptively transferred with CFSE-labeled, DO11.10 T cells and remained naive or were fed 100 mg OVA + 20 μg CT or 100 mg OVA. The behaviors of the TCR Tg, antigen-specific DO11.10 T cells in mesenteric (MLN; a, c, e, g, i, and k) and CLNs (PLN; b, d, f, h, j, and l) shown in Fig. 1 were analyzed in detail using PicViewer and Volocity software programs. The mean and standard error of volume (a and b), relative velocity (c and d), motility coefficient (e and f), and meandering index of representative cells ($n = 20$ –23 per group) are shown. The mean number of cells present in cell clusters (i and j) were determined from 10 time points and the mean number of cells per cluster was determined from the total

changes in the behavior of the T cells. Some of these changes were as described previously for T cells primed by exposure to antigen in PLNs draining a site immunized 48 h previously (9–11). In general, the number of antigen-specific T cells in the orally primed LNs increased (Fig. 1, c, f, i, and l), T cells undergoing priming appeared to slow down or stop (Videos 2, 5, 8, and 11, available at <http://www.jem.org/cgi/content/full/jem.20050203/DC1>) and some of the cells formed clusters (Fig. 1, c, f, i, and l and Videos 2, 5, 8, and 11). The clustering was typical of that seen when antigen-specific T cells contact an APC presenting their cognate antigen (7–15). The changes described were observed in MLNs at both 8 and 20 h after feeding antigen with adjuvant, though they were apparently more marked at the later time point (Fig. 1 f and Video 5). Similar changes in the behavior of antigen-specific CD4⁺ T cells were also observed in the CLNs, though they were perhaps more apparent 20 h after feeding (Fig. 1 l and Video 11). These observations indicate, for the first time, that antigen fed with the mucosal adjuvant CT affects T cells in local and systemic lymphoid organs, inducing changes in T cell behavior similar to those seen when antigen is coadministered with other adjuvants systemically (7–15). CT administered without antigen had no observable effect (unpublished data).

Observation of the induction of CD4⁺ T cell tolerance

In animals fed antigen alone, orally tolerized T cells also displayed dramatic changes in their behavior. Once again, and consistent with previous flow cytometric and immunohistochemical studies (2, 16, 17), the number of antigen-specific T cells in the orally tolerized LNs increased (Fig. 1, d, g, j, and m). These T cells also appeared to intermittently slow down or stop (Video 3, 6, 9, and 12, available at <http://www.jem.org/cgi/content/full/jem.20050203/DC1>) and many of the cells, though not as many as in priming, also formed clusters (Fig. 1, d, g, j, and m and Videos 3, 6, 9, and 12). Somewhat surprisingly, this pattern of behavior did not differ dramatically from that observed with oral priming. The alterations in behavior induced during tolerance induction were apparent in MLNs at both 8 and 20 h after feeding antigen, and again appeared more marked at the later time point (Fig. 1 g and Video 6). Similar changes in the behavior of antigen-specific T cells were also observed in CLNs, in contrast with oral priming, at both the 8- and 20-h time points after feeding (Fig. 1, j and m, and Videos 9 and 12). These observations indicate that antigen fed in a tolerogenic form affects

number of clusters identified in each condition as follows: k, MLN: 8 h; naive, $n = 26$; primed, $n = 48$; tolerized, $n = 45$; 20 h; naive, $n = 5$; primed, $n = 26$; tolerized, $n = 102$; and l (PLN): 8 h; naive, $n = 31$; primed, $n = 93$; tolerized, $n = 203$; 20 h; naive, $n = 18$; primed, $n = 24$; tolerized, $n = 33$). *, Significant differences ($P < 0.05$) between primed or tolerized and naive groups are indicated. †, Significant differences between primed and tolerized groups are shown. Replicate experiments were performed at the University of Strathclyde and at the University of California, Irvine with similar findings; those from the latter are shown.

T cell behavior (i.e., oral tolerance is not ignorance), that this occurs relatively rapidly and simultaneously in local and systemic lymphoid organs and that there are no overt, dramatic differences in the behavior of antigen-specific T cells underlying the outcome of oral priming versus oral tolerance.

Analysis of CD4⁺ T cell behavior during the induction of priming and tolerance

Differences in the behavior of antigen-specific T cells between oral priming and oral tolerance were not obvious from simple observation but became apparent after more detailed and quantitative analysis of LN images using a four-dimensional image display and analysis package developed locally (PicViewer).

Priming

We found that antigen-specific T cells in the CLNs had increased their volume to a similar extent (from $\sim 250 \mu\text{m}^3$ to $350 \mu\text{m}^3$) 8 h after feeding immunogenic or tolerogenic antigen (Fig. 2 b). The increase in T cell volume after antigen exposure is suggestive of blastogenesis and consistent with previous descriptions of the timing of T cell activation and division in oral priming and tolerance (2). This is the first analysis of this parameter by two-photon excitation microscopy, which provides a useful functional marker of activation and the changes here demonstrate that fed antigen was indeed having an effect. Confirmation of this data by flow cytometric analysis of forward scatter, or indeed reflection of the increase in cell density at these early time points has been inconclusive. Previous studies have demonstrated that this may reflect the problematic isolation of antigen-specific T cells from LNs for flow cytometry at early time points (<24 h) after antigen administration (20), and further emphasizes the importance of performing this type of study in a physiological *in vivo* system. The fact that this increase in volume was not detected in MLNs at any time point or CLNs at 20-h tissues probably reflects dynamic differences in the responses between tolerance and priming and local versus systemic lymphoid organs. Thus, blastogenesis may have occurred very rapidly in local tissues and is no longer apparent as cells have already divided, whereas cells in CLNs may have yet to divide at 20 h. Thus, as the peak response for any parameter may differ for each of these four scenarios (priming vs. tolerance in local vs. PLNs) very detailed time course studies will be required to address these issues in such dynamic interactions.

We next assessed the velocity of T cells in the conditions outlined above as previous studies have shown that this is reduced upon exposure to cognate antigen (7–15). Naive CD4⁺ T cells had a mean three-dimensional velocity of $15 \mu\text{m min}^{-1}$, which broadly agrees with previous estimates of $10 \mu\text{m min}^{-1}$ (7–15). This minor difference may reflect that previous studies have assessed velocity in two dimensions (X and Y), rather than the three dimensions (X, Y, and Z) used here. As with cells primed by other routes, orally primed cells had a significantly reduced mean velocity compared

with naive cells (Fig. 2, c and d). It is important to note that the determination of the velocity of these cells excluded those in clusters. The reduction in velocity observed in oral priming could be the result of an overall slowing of all primed T cells and/or a marked slowing (stopping) of a proportion of the cells. Furthermore, the velocity obtained would be further reduced if cells in clusters, which are essentially stopped, were included in this analysis.

Previous studies have demonstrated that in addition to changes in velocity, primed T cells also undergo changes in movement behavior, with naive cells exhibiting a “random walk” pattern and primed cells undergoing nonrandom movement (7–15). The long-term rate of T cell displacement is governed by the random walk of the cell as well as its instantaneous velocity and is characterized by the cell motility coefficient (M; reference 9). Analogous to the diffusion coefficient of a molecule, M relates the displacement (d) of the cell from a starting point with time (t),

$$d = \sqrt{6Mt},$$

and is computed from the slope of a plot of displacement versus square root time along a measured T cell path.

As with previous studies, orally primed T cells had a lower motility coefficient than naive cells, possibly reflecting a less random movement (Fig. 2, e and f). However, this could also be the result of reduced velocity and/or cells stopping intermittently for short periods.

To determine if this change in movement could be explained by an increase in how convoluted the T cell paths were, we determined a meandering index. This was computed as the ratio of the distance between the initial and final points on each T cell track divided by the total length of the random path, with a linear track therefore having an index of 1. No significant differences in meandering index were detected (Fig. 2, g and h).

Despite the fact that we routinely scanned a large number of closely apposed planes at high speed, difficulties in consistently identifying individual cells within T cell clusters were encountered and it remains formally possible that cells entered or left clusters unobserved in this period. Furthermore, as their inclusion would artificially bias results, the aforementioned analyses were derived from cells that were not part of the clusters apparent in Fig. 1. As the size of cluster and the number of cells involved in forming clusters appeared to vary between conditions, we therefore computed these parameters for each cluster, as described in Materials and methods. Only a relatively low proportion of cells was associated with clusters in naive mice (Fig. 2, i and j), and these clusters were small (Fig. 2, k and l). The proportion of cells in clusters was significantly increased in primed animals by 20 h in MLNs and 8 h in CLNs (Fig. 2, i and j) and importantly, this was associated with a significant increase in the number of cells per cluster at 20 h that was particularly evident in MLNs (Fig. 2, k and l). CT administered without

antigen had no apparent effect on these parameters (unpublished data).

Tolerance

At face value, tolerized T cells displayed a behavior similar to that of primed T cells. However, detailed analysis revealed that though their velocity, motility coefficient, and mean-dering index were not significantly different to those of

primed T cells (Fig. 2, c–h), cell clustering was clearly different (Fig. 2, i–l). Although the proportion of tolerized T cells participating in clusters in MLNs was not different when comparing priming and tolerance (Fig. 2, i and j), the numbers of cells within each cluster was significantly less in tolerance compared with priming (Fig. 2, k and l). In CLNs, a significantly higher proportion of cells in tolerized animals were involved in clusters at 8 h (Fig. 2 j). However, it should

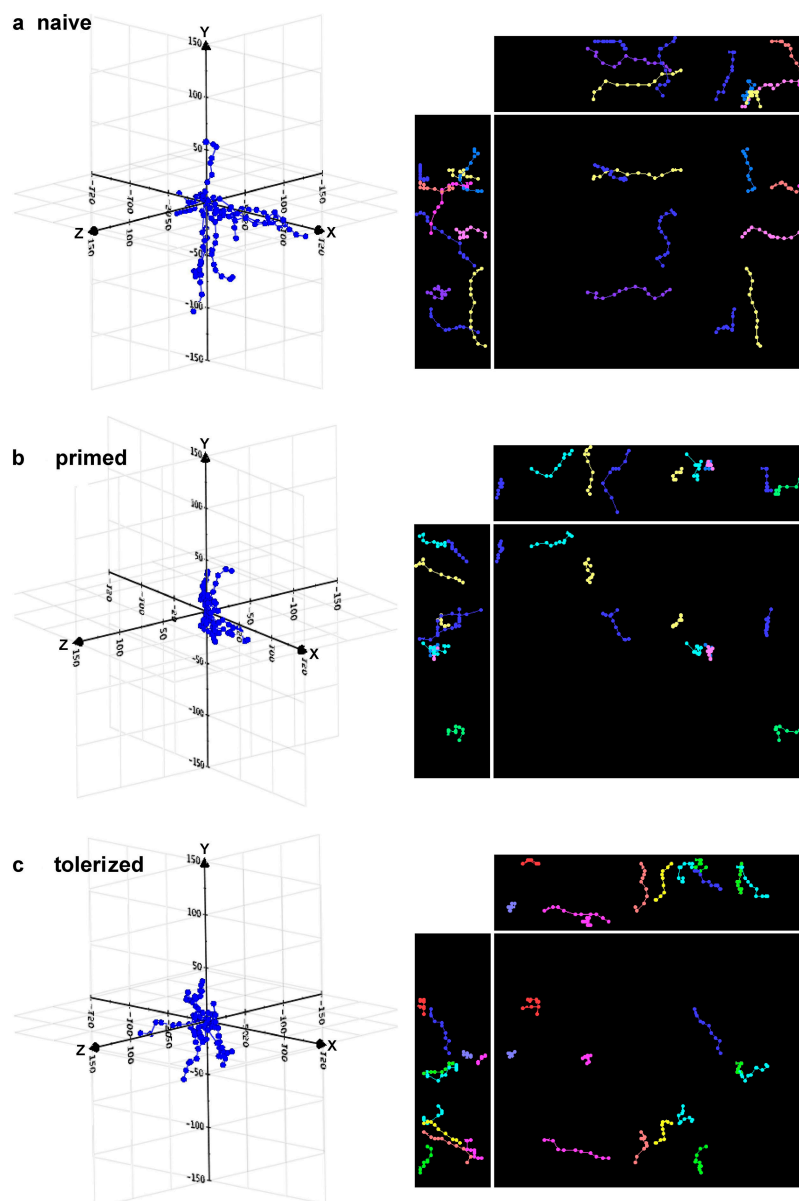


Figure 3. Analysis of the behavior of antigen-specific T cells in MLNs during the induction of oral priming and tolerance. As described in Fig. 1, BALB/c mice were adoptively transferred with CFSE-labeled DO11.10 T cells and remained naive or were fed 100 mg OVA + 20 μ g CT or 100 mg OVA. The behaviors of the TCR Tg, antigen-specific DO11.10 T cells in mesenteric and cervical LNs shown in Fig. 1 were analyzed in detail using Velocity software. Plots representative of the relative

and absolute movement of naive (a), primed (b), and tolerized (c) T cells in MLN 20 h after antigen administration are shown. Each plot was produced using Velocity software and displays 10 three-dimensional tracks over 10–14 time points, separated by 18 s per time point. Replicate experiments were performed at the University of Strathclyde and at the University of California, Irvine with similar findings; those from the latter are shown.

be noted that the number of cells per cluster was very small, usually containing only two cells (Fig. 2 l), and could therefore be a result of increased numbers of random collisions between labeled cells due to their increased frequency.

These analyses were confirmed with Volocity software (Improvision; not depicted) and representative tracks from a naive, primed, or tolerized CD4⁺ T cell are shown in Fig. 3. Interestingly, this analysis exaggerated some of the differences noted (e.g., meandering index) as it includes cells within clusters.

In vivo observation and confirmation of CD4⁺ T cell priming and tolerance

To confirm that our observations of T cells in oral priming and tolerance in ex vivo LNs were truly reflective of the physiological situation in vivo, we performed direct intravital analyses (Videos 13 and 14, available at <http://www.jem.org/cgi/content/full/jem.20050203/DC1>). These studies confirmed earlier work by showing that T cells in LNs in situ behaved the same as those in excised LNs. Thus, naive T cells move relatively quickly within LNs (~12 $\mu\text{m}/\text{min}$ compared with 15 $\mu\text{m}/\text{min}$ for excised) in a random manner and do not cluster (Videos 13 and 14). In contrast, antigen-exposed T cells, both primed and tolerized, slow down (velocity reduced to ~5 $\mu\text{m}/\text{min}$ and 7 $\mu\text{m}/\text{min}$, respectively, compared with 10 $\mu\text{m}/\text{min}$ for excised) or stop and exhibit clustering (Videos 13 and 14). These analyses (Fig. 4) confirmed our ex vivo findings and, as they were performed on inguinal LNs, also confirmed the effects of orally delivered antigen on T cells in peripheral lymphoid organs (Videos 13 and 14).

The expected effects of oral priming and tolerance on T cell behavior were confirmed by flow cytometry. As described previously (2, 16–19), in animals fed OVA in immunogenic or tolerogenic forms, antigen-specific T cells up-regulated the expression of CD69 (Fig. 4 b) and divided (Fig. 4, c–f), although this was decreased in tolerance when compared with priming. Finally, as reported previously (2, 16–19), primed animals displayed an enhanced serum anti-OVA IgG1 response to systemic challenge that was suppressed in tolerized animals when compared with controls (Fig. 4 g).

DISCUSSION

Understanding the mechanisms and requirements for the induction of immunological priming versus tolerance of CD4⁺ T cells will be critical for the development of vaccines against pathogens and therapies for the treatment of autoimmune diseases. Although it has been suggested that differences in the behavior of CD4⁺ T cells during interactions with APCs may underlie the differential outcome of priming versus tolerance, this has not been examined directly in vivo.

We have examined, for the first time, the behavior of T cells during the induction and evolution of priming and tolerance in local, gut draining, and systemic LNs in a physiologically relevant model of immunoregulation to fed antigen. We find that there are no differences between primed

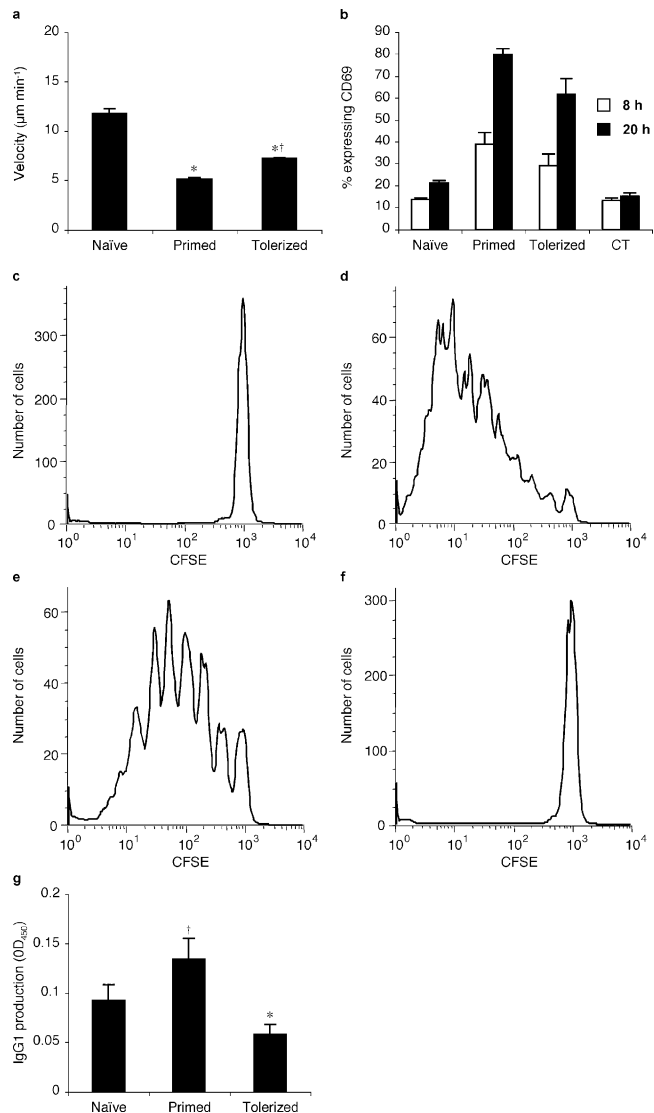


Figure 4. Intravital analysis of the behavior of antigen-specific T cells in inguinal LNs during the induction of oral priming and tolerance and confirmation of the induction of priming versus tolerance.

As described in Fig. 1, BALB/c mice were adoptively transferred with CFSE-labeled DO11.10 T cells and remained naive or were fed 100 mg OVA + 20 μg CT or 100 mg OVA. The velocity (a) of the TCR Tg, antigen-specific DO11.10 T cells in inguinal LNs in situ were analyzed in detail using PicViewer software. The mean and standard error of relative velocity are shown. The CD69 expression (b) and division of naive (c), primed (d), tolerized (e), and CT exposed (f) TCR Tg T cells is shown, as is the OVA-specific IgG1 in response to challenge (g). *, Significant differences ($P < 0.05$) between primed or tolerized and naive groups are indicated. †, Significant differences between primed and tolerized groups are shown.

and tolerized T cells in their speed and form of movement, but that apparently minor increases in the size and persistence of T cell clusters underlies the induction of priming versus tolerance. There was an apparent increase in the proportion of cells participating in clusters in tolerance, but it should be noted that the number of cells per cluster was very

small, usually containing only two cells and could therefore be a result of increased numbers of random collisions between labeled cells due to their increased frequency. In any given snapshot of the three-dimensional imaged volume within the LN, a certain amount of cell clustering is expected to occur purely due to random collisions between free-moving cells, with the number of such clusters increasing with cell density. To determine whether the observed clustering in our experiments could be explained by these random encounters alone, we computed the expected number and size of clusters arising from random collisions, for given cell densities, average cell volume, and image volume. A simple Monte-Carlo simulation was used with cells placed randomly and clusters identified by the presence of cells in adjacent grid points. Comparison of the predicted versus actual data demonstrated that, on exposure to antigen, the increase in percent cells in cluster and number of cells per cluster is not a result of increased cell density; i.e., actual clustering is always greater than predicted upon exposure to antigen, whereas this is not the case with naive cells (Table S1, available at <http://www.jem.org/cgi/content/full/jem.20050203/DC1>). These findings indicate a subtle difference in behavior with tolerized T cells forming a greater number of smaller clusters than primed T cells, which participate in fewer, larger, and long-lived clusters. Thus, tolerized T cells may have either a wider orbit of interest or, more likely, a lesser focus on a particular nidus of attention. It will be important to determine whether differences in cluster size are a result of changes in duration of interaction, which could reflect alterations in off-rate, on-rate, or both. It should now also be possible to investigate, at the molecular level, whether these differences are a result of changes in the T cell, the APC, or both.

It is interesting to note that, as with recent studies of CD8⁺ T cell tolerance (14), the events we observe in tolerance and priming are generally similar at early time points (8 h), but diverge later (20 h) when priming is associated with larger, longer-lived, more stable clusters. In particular, the largest clusters were observed in the MLNs 20 h after oral priming. The differences in the timing and location of the changes in T cell behavior in oral priming versus oral tolerance reflect the effects of the adjuvant, CT. Consistent with previous papers (21–23), it seems likely that this causes an initial acquisition and subsequent slower, sustained presentation of antigen than tolerance, where large quantities of antigen are available throughout the animal very quickly after feeding in the absence of adjuvant. Alternatively, there may be differential levels or maintenance of antigen presentation, costimulation, and/or recruitment of different APC populations that sustain presentation, as recently observed in systemic priming (24).

Although differences between priming and tolerance were more marked in mucosal lymphoid organs, similar changes were observed simultaneously in systemic lymphoid tissues.

Importantly, we characterized the behavior of T cells resident in the LN within a short time of exposure to anti-

gen. In previous studies, animals were immunized some time (48 h) before adoptive transfer to synchronize the behavior of the T cells under study and assess their behavior during the establishment of immunity (9). Alternatively, for similar reasons, some studies have altered the normal “ebb and flow” of T cells through a LN (8). As we aimed to determine if differences in early interactions underlie the decision of T cells to become primed or tolerized and as the nature of antigen presentation changes dramatically as DCs mature (25) and other APCs (e.g., antigen-specific B cells) become involved (26, 27), we transferred T cells before antigen feeding. This approach is more challenging, as the behavior of the T cells is not synchronized, though significantly it may be more reflective of the true physiological situation during the early induction phases of immune responses.

It should be kept in mind that, although our analyses are as detailed as any previous study, as with all such approaches, they are still limited by the number of cells and fields of cells that can be examined in any LN, as well as the location of the field of view, and the fact that TCR transgenic (Tg) T cells and their adoptive transfer may not be reflective of the physiological situation. With these caveats, two-photon excitation microscopy is now established as an important tool for immunological research, but it will be the interpretation and analysis of images that will be important and revealing (28, 29). Indeed, our detailed analyses of tolerance versus priming have demonstrated that a major difference in immunological outcome of antigen administration, as demonstrated by comparisons of CD69 expression, division and antibody responses to challenge, may be a result of subtle changes in behavior that are not immediately apparent by observation alone.

In conclusion, we have presented the first two-photon excitation characterization of antigen-specific CD4⁺ T cells *in vivo*, in real time, during the induction of oral priming versus oral tolerance. Our studies have shown that dramatic changes in T cell behavior occur simultaneously in local (MLN) and peripheral (CLN) lymphoid organs after oral administration of antigen with or without adjuvant. The differences in cell behavior between these two regimes, that have such different outcomes at a gross immunological level, were however relatively minor and subtle. These changes may be a consequence of variations in the expression of molecules such as chemokines, cytokines, costimulatory molecules, and their receptors and it will be important to define these differences using technologies such as targeted and inducible reporters and dominant negatives to visualize and modify cell functions. It will also be interesting to investigate other tolerizing regimes where different mechanisms of tolerance may occur (e.g., deletion, anergy, T reg cell) and examine the behavior of primed and tolerized T cells after challenge when functional priming and tolerance is observed. These findings will have important implications for the design, targeting, and application of vaccination and immunotherapeutic strategies in general, but particularly those delivered via mucosal tissues.

MATERIALS AND METHODS

Animals. Mice homozygous for the cOVA peptide₃₂₃₋₃₃₉/I-A^d-specific DO11.10 TCR transgenes on the BALB/c background were used as T cell donors (30). 6-wk-old BALB/c (H-2^b) mice were purchased from Harlan-Olac and were used as recipients. All animals were specified pathogen free and were maintained under standard animal house conditions in accordance with local and Home Office regulations.

Preparation of cell suspensions for adoptive transfer. PLNs (axillary, inguinal, cervical), MLNs, and spleens from DO11.10 mice were pooled and forced through Nitex mesh (Cadisch Precision Meshes) using a syringe plunger. Suspensions were washed in RPMI 1640 (GIBCO BRL). CD4⁺ cells were purified by negative selection with anti-CD8, anti-CD19, anti-CD11b, and anti-CD16/32 over MACS columns (Miltenyi Biotec) as described previously (9–11). The CD4⁺ KJ1.26⁺ T cell percentage was determined by flow cytometric analysis as described previously (9–11).

CFSE labeling of Tg lymphocytes and assessment by flow cytometry. Cell suspensions were prepared as described in the previous paragraph before being washed 2× in HBSS (Sigma-Aldrich) and resuspended at a concentration of 5×10^7 lymphocytes/ml. Cells were incubated with 5-(and-6-)carboxyfluorescein diacetate, succinimidyl ester (5(6)-CFDA, SE; Molecular Probes Inc.) at 10^7 cells per ml HBSS + 0.5 μl of 10 mM CFSE stock solution in DMSO for 15 min at 37°C.

Cells were washed in HBSS, then with complete medium (RPMI 1640, 10% FCS, 2 mM L-glutamine, 100 U/ml penicillin, 100 mg/ml streptomycin, 1.25 mg/ml fungizone; all obtained from GIBCO BRL) before resuspending at $2-5 \times 10^6$ Tg cells/adoptive transfer. Tg T cells were injected i.v. into age- and sex-matched BALB/c recipients as described previously (17).

The activation of TCR Tg T cells (CD69 expression and cell division history) was assessed by flow cytometry as described previously (2, 16–19).

Antigen administration. Chicken OVA (fraction V) and CT were obtained from Sigma-Aldrich. After adoptive transfer, recipient mice were sham treated with PBS or exposed to antigen by feeding with 100 mg OVA, or 100 mg OVA with 20 μg CT (OVA/CT; Sigma-Aldrich) as described previously (2, 16). These regimes have consistently resulted in oral tolerance or oral priming (2, 16). In challenge experiments, animals were immunized s.c. with 100 μg OVA in 50 μl CFA 10 d after feeding and serum anti-OVA IgG1 levels determined 21 d later by ELISA as described previously (2, 16–19).

Two-photon excitation microscopy. Excised or in situ mesenteric and PLNs were imaged essentially as described previously (9–11). The excised LN was transferred into CO₂-independent medium (GIBCO BRL) at room temperature. The LN was bound (Vetbond, 3M) on a coverslip. The coverslip was adhered with grease to the bottom of the imaging chamber that was continuously supplied with warmed (37°C) and gassed (95% O₂ and 5% CO₂) medium (RPMI 1640 with 25 mM Hepes) before and throughout the period of microscopy.

Two-photon microscopy was performed as described previously (9–11), alternatively imaging was performed as described in the next paragraph. The two-photon excitation source was an all-solid-state, tuneable Titanium: sapphire laser system (5W Verdi/Mira 900F, Coherent Laser Group). The laser pulse duration and sample pulse duration were measured with an optical autocorrelator (Carpe, APE). The laser beam was routed into a multiphoton excitation laser scanning system (MRC-1024MP, Bio-Rad Laboratories). The scan head was aligned through an upright microscope (E600-FN; Nikon). The objective lens used for all imaging investigations was the CFI-60 Fluo-W 40X/0.8 NA water-dipping objective lens (Nikon). The sample was illuminated with 780 nm, ~210 fs pulse duration and 76 MHz repetition frequency. In addition, during the imaging, the average power was remotely monitored by a Silicon photo-diode and the peak power was monitored by a GaAsP planar diffusion photo-diode (S2844K, G1116; Hamamatsu Photonics).

The excited fluorescence passed through a laser blocking filter (E625SP; Chroma Technologies) and was detected with a multi-alkali cathode photo-multiplier tube (S20 PMT) in an external or nondescanned configuration as part of the MRC-1024MP system. The emission spectrum detected was 420 nm to 620 nm or, alternatively, from 500 to 550 nm with an additional emission filter (HQ525/50; Chroma Technologies). The scans were acquired with 500 fps and 256×256 -pixel boxes, for a frame rate of 1.95 fps. The image pixel size was 0.55 μm with 5.2 μs pixel dwell time. Each imaged volume consisted of ~21 planes 2.5 μm apart. The volumes were acquired every 18 s apart for the time indicated.

Analysis and statistics. The volume and location (centroid) of T cells within each three-dimensional image stack were determined using an intensity threshold-based object detection algorithm that automatically located and classified all discrete blocks of contiguous voxels exceeding a fixed intensity. T cell movements were tracked in three dimensions by visual identification of individual T cell objects within extended focus projections of successive stacks and manual selection by the operator. Only T cell tracks with at least nine time points were included in the analysis. Instantaneous T cell velocity was computed as the distance between centroids of the T cell objects in successive stacks divided by the interstack time interval.

Clusters were identified when two cells or more could not be separated by PicViewer. Detected objects with volumes in the range of 540–750 μm³ were considered to be clusters of two cells. For objects with a volume >750 μm³, the number of cells per clusters was determined by dividing the object volume by 300 μm³.

Results are expressed as mean ± SEM or mean + range. Analysis of variance (with Tukey multiple comparison tests) was used to determine the statistical significance of differences between naive, primed, and tolerized groupings of results, a p-value of 0.05 was regarded as significant.

Online supplemental material. Video 1 shows that naive, OVA-specific T cells in MLNs display a random walk behavior. Video 2 demonstrates that 8 h after priming, OVA-specific T cells in MLNs have reduced velocity and formed clusters. Video 3 illustrates that tolerized, OVA-specific T cells in MLNs display similar behavior to primed cells at 8 h. Video 4 indicates the random walk behavior of naive, OVA-specific T cells in MLNs at 20 h. Video 5 shows the pronounced reduction in velocity and cluster formation of primed, OVA-specific T cells in MLNs at 20 h versus 8 h. Video 6 shows that tolerized, OVA-specific T cells appear to form smaller and more transient clusters than primed cells in MLNs at 20 h. Video 7 displays the random walk behavior of naive, OVA-specific T cells in CLNs. Video 8 demonstrates that primed, OVA-specific T cells in CLNs have reduced velocity and formed small transient clusters. Video 9 illustrates that tolerized, OVA-specific T cells in CLNs display similar behavior to primed cells 20 h after antigen administration. Video 10 shows naive, OVA-specific T cells in CLNs display a random walk behavior. Video 11 shows that primed, OVA-specific T cells in CLNs have reduced velocity and formed clusters, though not as pronounced as in MLNs. Video 12 demonstrates that tolerized, OVA-specific T cells in CLNs appear to form smaller and more transient clusters than primed cells. Video 13 reveals similar changes in behavior between primed and naive cells as observed in explanted CLNs occurs in inguinal LNs in situ. Video 14 shows intravital analysis of OVA-specific T cells in inguinal LNs revealing similar changes in behavior between tolerized and naive cells as observed in explanted CLNs. Table SI demonstrates that random collisions as a result of increased cell density does not explain either the increase in percent cells clustering or number of cells per cluster observed in primed or tolerized versus naive cells. Online supplemental material is available at <http://www.jem.org/cgi/content/full/jem.20050203/DC1>.

The authors wish to thank Mr. R. Oxland for excellent technical assistance.

This work was supported by a Wellcome Trust grant no. 068895 (awarded to P. Garside, J.M. Brewer, A.M. Gurney, and D. Wokosin) and National Institutes of Health grant nos. GM-41514 (to M. Cahalan) and GM-48071 (to I. Parker).

The authors have no conflicting financial interests.

Submitted: 25 January 2005

Accepted: 19 April 2005

REFERENCES

- Kearney, E.R., K.A. Pape, D.Y. Loh, and M.K. Jenkins. 1994. Visualisation of peptide-specific T cell immunity and peripheral tolerance induction in vivo. *Immunity*. 1:327–339.
- Smith, K.M., J.M. Davidson, and P. Garside. 2002. T-cell activation occurs simultaneously in local and peripheral lymphoid tissue following oral administration of a range of doses of immunogenic or tolerogenic antigen although tolerized T cells display a defect in cell division. *Immunology*. 106:144–158.
- Dustin, M.L. 2004. Stop and go traffic to tune T cell responses. *Immunity*. 21:305–314.
- Sumen, C., T.R. Mempel, I.B. Mazo, and U.H. von Andrian. 2004. Intravital microscopy: visualizing immunity in context. *Immunity*. 21:315–329.
- Huang, A.Y., H. Qi, and R.N. Germain. 2004. Illuminating the landscape of in vivo immunity: insights from dynamic in situ imaging of secondary lymphoid tissues. *Immunity*. 21:331–339.
- Friedl, P., and M. Gunzer. 2001. Interaction of T cells with APCs: the serial encounter model. *Trends Immunol.* 22:187–191.
- Mempel, T.R., M.L. Scimone, J.R. Mora, and U.H. von Andrian. 2004. In vivo imaging of leukocyte trafficking in blood vessels and tissues. *Curr. Opin. Immunol.* 16:406–417.
- Mempel, T.R., S.E. Henrickson, and U.H. Von Andrian. 2004. T-cell priming by dendritic cells in lymph nodes occurs in three distinct phases. *Nature*. 427:154–159.
- Miller, M.J., S.H. Wei, I. Parker, and M.D. Cahalan. 2002. Two-photon imaging of lymphocyte motility and antigen response in intact lymph node. *Science*. 296:1869–1873.
- Miller, M.J., S.H. Wei, M.D. Cahalan, and I. Parker. 2003. Autonomous T cell trafficking examined in vivo with intravital two-photon microscopy. *Proc. Natl. Acad. Sci. USA*. 100:2604–2609.
- Miller, M.J., O. Safirina, I. Parker, and M.D. Cahalan. 2004. Imaging the single cell dynamics of CD4⁺ T cell activation by dendritic cells in lymph nodes. *J. Exp. Med.* 200:847–856.
- Cahalan, M.D., I. Parker, S.H. Wei, and M.J. Miller. 2002. Two-photon tissue imaging: seeing the immune system in a fresh light. *Nat. Rev. Immunol.* 2:872–880.
- Cahalan, M.D., I. Parker, S.H. Wei, and M.J. Miller. 2003. Real-time imaging of lymphocytes in vivo. *Curr. Opin. Immunol.* 15:372–377.
- Hugues, S., L. Fetler, L. Bonifaz, J. Helft, F. Amblard, and S. Amigorena. 2004. Distinct T cell dynamics in lymph nodes during the induction of tolerance and immunity. *Nat. Immunol.* 5:1235–1242.
- Bouso, P., and E. Robey. 2003. Dynamics of CD8(+) T cell priming by dendritic cells in intact lymph nodes. *Nat. Immunol.* 4:579–585.
- Smith, K.M., F. McAskill, and P. Garside. 2002. Orally tolerized T cells are only able to enter B cell follicles following challenge with antigen in adjuvant, but they remain unable to provide B cell help. *J. Immunol.* 168:4318–4325.
- Millington, O.R., A.M. Mowat, and P. Garside. 2004. Induction of bystander suppression by feeding antigen occurs despite normal clonal expansion of the bystander T cell population. *J. Immunol.* 173:6059–6064.
- Williamson, E., G.M. Westrich, and J.L. Viney. 1999. Modulating dendritic cells to optimize mucosal immunization protocols. *J. Immunol.* 163:3668–3675.
- Sun, J., B. Dirden-Kramer, K. Ito, P.B. Ernst, and N. Van Houten. 1999. Antigen-specific T cell activation and proliferation during oral tolerance induction. *J. Immunol.* 162:5868–5875.
- Maxwell, J.R., R.J. Rossi, S.J. McSorley, and A.T. Vella. 2004. T cell clonal conditioning: a phase occurring early after antigen presentation but before clonal expansion is impacted by Toll-like receptor stimulation. *J. Immunol.* 172:248–259.
- Holmgren, J., A.M. Harandi, and C. Czerkinsky. 2003. Mucosal adjuvants and anti-infection and anti-immunopathology vaccines based on cholera toxin, cholera toxin B subunit and CpG DNA. *Expert Rev. Vaccines*. 2:205–217.
- Holmgren, J., C. Czerkinsky, K. Eriksson, and A. Mharandi. 2003. Mucosal immunisation and adjuvants: a brief overview of recent advances and challenges. *Vaccine*. 21:S89–S95.
- Lycke, N. 1997. The mechanism of cholera toxin adjuvanticity. *Res. Immunol.* 148:504–520.
- Itano, A.A., S.J. McSorley, R.L. Reinhardt, B.D. Ehst, E. Ingulli, A.Y. Rudensky, and M.K. Jenkins. 2003. Distinct dendritic cell populations sequentially present antigen to CD4 T cells and stimulate different aspects of cell-mediated immunity. *Immunity*. 19:47–57.
- Gett, A.V., F. Sallusto, A. Lanzavecchia, and J. Geginat. 2003. T cell fitness determined by signal strength. *Nat. Immunol.* 4:355–360.
- Garside, P., E. Ingulli, R.R. Merica, J.G. Johnson, R.J. Noelle, and M.K. Jenkins. 1998. Visualization of specific B and T lymphocyte interactions in the lymph node. *Science*. 281:96–99.
- Smith, K.M., J.M. Brewer, C.M. Rush, J. Riley, and P. Garside. 2004. In vivo generated Th1 cells can migrate to B cell follicles to support B cell responses. *J. Immunol.* 173:1640–1646.
- Witt, C., S. Raychaudhuri, and A.K. Chakraborty. 2005. Movies, measurement, and modeling: the three Ms of mechanistic immunology. *J. Exp. Med.* 201:501–504.
- Tarakhovskiy, A. 2005. On imaging, speed, and the future of lymphocyte signaling. *J. Exp. Med.* 201:505–508.
- Murphy, K.M., A.B. Heimberger, and D.Y. Loh. 1990. Induction by antigen of intrathymic apoptosis of CD4⁺CD8⁺TCR^{lo} thymocytes in vivo. *Science*. 250:1720–1723.